Application of Long Short-Term Memory Neural Network and Prophet Algorithm in Slope Displacement Prediction

Libin Tang, *School of Civil Engineering, Chongqing University, Chongqing 400045, China; email: tanglibin@cqu.edu.cn*
Yanbin Ma, *School of Civil Engineering, Chongqing University, Chongqing 400045, China; email: myb0919@163.com*
Lin Wang, *Assistant Professor, School of Civil Engineering, Chongqing University, Chongqing 400045, China; email: sdxywanglin@cqu.edu.cn*
Wengang Zhang, *School of Civil Engineering, Key Laboratory of New Technology for Construction of Cities in Mountain Area, National Joint Engineering Research Center of Geohazards Prevention in the Reservoir Areas, Chongqing University, Chongqing 400045, China; email: zhangwg@cqu.edu.cn*
Lining Zheng, *China Southwest Geotechnical Investigation and Design Institute Co., Ltd; email: zhengning2003@163.com*
Haijia Wen, *School of Civil Engineering, Chongqing University, Chongqing 400045, China; email: jhw@cqu.edu.cn*

ABSTRACT: *The slope displacement prediction is crucial for the development of an early warning system, which can help prevent or reduce losses of lives, properties, and the local environment. This problem is particularly important in the Three Gorges Reservoir (TGR) area, where the influence of geological, weather, and hydraulic conditions on landslides is significant. It is generally acknowledged that reservoir landslides are complex nonlinear systems with dynamic and inter-related features. However, most studies focus on how to express the static relationships between triggering factors and the landside displacement. In this paper, a long short-term memory (LSTM) neural network model was applied for predicting the total displacement of the Bazimen landslide, based on the decomposition of displacement time series.*

The accumulated displacement can be divided into two main parts: the trend and the periodic terms. The long-term trend was fit with a cubic nonlinear regression model; the residual one (the periodic displacement) was predicted via the LSTM model. By analyzing historical information and the Pearson correlation coefficient, a dynamic model was developed using six controlling factors. The good consistency between the predicted and monitored data proves the superiority of the model in predicting dynamic time-series problems. Compared with conventional static methods (i.e., MARS and SVM), the LSTM model can make full use of historical information due to its special "memory" structure. However, all these three methods can only perform well in forecasting one-step problems. To meet the requirement of multi-step forecasting, the Facebook Prophet model was also used in this study to predict landslide displacements with a longer period. The predicted results demonstrate the model's superiority in efficiency and practice, at a cost of prediction accuracy.

KEYWORDS: Slope Displacement, Long Short-Term Memory, Neural Network, Prophet Algorithm, TGR, Predictive Accuracy

SITE LOCATION: Geo-Database

INTRODUCTION

China is one of the countries with the most serious geological disasters in the world (Wang et al., 2004; Keqiang et al., 2008; Li et al., 2010; Du et al., 2013). In some cases, landslides can cause huge losses in human lives and properties as well as impose significant impacts on the environment (Yin et al., 2010; Zhang et al., 2020a). Specifically, due to the complex geological conditions associated with high mountain areas and intensive human engineering activities, landslides occur

Submitted: 31 October 2020; Published: 25 October 2021
Reference: Tang L., Ma Y., Wang L., Zhang W., Zheng L., and Wen H. (2021). Application of Long Short-Term Memory Neural Network and Prophet Algorithm in Slope Displacement Prediction. International Journal of Geoengineering Case Histories, Volume 6, Issue 4, pp. 48-66, doi: 10.4417/IJGCH-06-04-04

frequently in the Three Gorges Reservoir (TGR) region, where steep slopes exist and flooding often occurs (Xu and Niu, 2018; Xie et al., 2019). The Qianjiangping landslide on 13 July 2003 destroyed 4 factories and 129 houses, caused 24 deaths, and rendered more than 1,000 people homeless (Jian et al., 2014). It is one of the most devastating landslides in the TGR, as it occurred shortly after the first impoundment of the reservoir (Wang et al., 2004; Jian et al., 2014).

It has been well acknowledged that the coupling effect of seasonal rainfall and periodic fluctuation of the reservoir water level poses a great threat to slope safety (Li et al., 2010; Du et al., 2013; Cao et al., 2016; Huang et al., 2017; Yang et al., 2019; Chen et al., 2020; Wang et al., 2020a; Zhang et al., 2020a). However, landslides are complex dynamic and nonlinear systems, and their failure mechanisms have not been fully explored by researchers (Xu and Niu, 2018). In recent decades, in order to better control disaster risks and issue early warnings, monitoring networks and controlling systems have been widely used in landslide-prone areas (Li et al., 2010). Based on the large amount of recorded data, it is possible to analyze the complex relationships between the landslide displacement and its triggering factors. The accuracy of the landslide displacement prediction model depends on how these complex relationships are expressed and reflected (Xu and Niu, 2018; Yang et al., 2019).

Conventional landslide displacement approaches such as physical experiments, numerical analysis, and empirical formulas have certain advantages yet also disadvantages (Huang et al., 2017; Xu and Niu, 2018; Yang et al., 2019). For example, laboratory experiments perform well in revealing the landslide evolution and enhance the understanding on the failure mechanisms, e.g., based on the creep theory and soil and rock mechanics. On the other hand, these experiments are costly and require more time and effort when compared with numerical simulations. Recently, with the development of artificial intelligence, numerous data-driven models have been used for landslide displacement prediction (Li et al., 2010; Du et al., 2013; Zhou et al., 2016; Huang et al., 2017; Zhou et al., 2018; Xie et al., 2019; Yang et al., 2019). Compared with the above methods, the data-driven models are gaining increasing popularity because they achieve a balance between computational costs and model accuracy (Lian et al., 2015; Wang et al., 2020b; Zhang et al., 2020b). Therefore, it can be inferred that a combination of conventional approaches and artificial intelligence methods will be much more applicable for landslide problems in the future.

There are two main categories of artificial intelligence methods applied to the prediction of landslide displacement: the ones considering comprehensive effects of triggering factors, and others considering the landslide displacement itself (Xu and Niu, 2018). Among these methods, artificial neural networks (ANNs), extreme learning machines (ELMs), and support vector machines (SVMs) are commonly used to predict the landslide displacement (Du et al., 2013; Lian et al., 2015; Cao et al., 2016; Zhou et al., 2016; Zhou et al., 2018). For instance, Du et al. (2013) used the back-propagation neural network (BPNN) method to predict the landslide displacement, with the time-series models. Cao et al. (2016) proposed an extreme learning machine model to analyze the displacement characteristics, with a time-series expression. Zhou et al. (2016) compared the predicted displacements of an improved SVM model and the BPNN method, decomposing the displacement time series. These examples illustrate how the combination of time-series analysis and machine learning methods to predict landslide displacement is becoming increasingly popular.

Using a time-series model, the landslide displacement is divided into two main parts: the long-term trend primarily controlled by internal factors (i.e., geological conditions and material properties) and the periodic displacement significantly affected by external factors (i.e., rainfall and reservoir water level). The long-term trend is more time-dependent and grows gently, and it can be fit by a polynomial function with high accuracy. Regarding the periodic term, its periodicity is closely related to seasonal rainfall and regular reservoir scheduling, and thus predicting it is more complex (Du et al., 2013; Xu and Niu, 2018; Yang et al., 2019).

More recently, the long short-term memory (LSTM) model has gained a lot of attention because it can efficiently reflect dynamic responses of the landslide displacement under the coupling effect of rainfall and reservoir water level (Xing et al., 2019; Zhang et al., 2019; Jiang et al., 2020). The LSTM model was first proposed by Hochreiter and Schmidhuber (1997), and can be considered as an improved method of the recurrent neural network (RNN) (Sak et al., 2014) which uses a special "memory" structure to better control and judge historical information. For instance, Fan et al. (2014) investigated the use of the LSTM model for TTS speech synthesis. Weytjens et al. (2019) found that the LSTM model is particularly useful for time-series forecasting, as compared with classical predictive methods such as ARIMA. Kong et al. (2017) efficiently used the LSTM model for handling the short-term load forecasting problem of individual residential households.

The LSTM model has been proven to be a reliable method for building other forecasting models in many previous studies, including landslide displacement prediction problems. For instance, Zhang et al. (2019) found that the LSTM model performs

better in predicting landslide displacements than the SVM and the Elman neural network (ENN) models, although it needs more time for training. Yang et al. (2019) compared the predicted displacements of the SVM and LSTM models respectively, and verified the higher accuracy of the latter. Xing et al. (2019) proposed an improved LSTM model through the stacking of neural network layers, and it has been successfully applied to the Dashuitian landslide in China. However, the performance the LSTM model on landslide displacement prediction still needs to be explored and improved through more case studies.

In this work, the LSTM model was adopted to predict landslide displacements of the Bazimen landslide in the TGR area, based on a time-series analysis and triggering factors selection. The implementation of the predictive model comprises four main tasks: (1) decomposing the total displacements into the trend term and the periodic term; (2) using a nonlinear regression function to fit the trend term; (3) building the model to predict periodic displacements by analyzing the relationships between periodic displacements and rainfall and the reservoir water level; and (4) adding the predicted trend and periodic displacements as the predicted total displacements. The SVM, MARS, and the Prophet models are also used to verify the results and compare the model performance.

METHODOLOGY

Machine Learning Methods

Recurrent Neural Network

The recurrent neural network (RNN) is an expansion of the artificial neural network (ANN), which aims to mimic the processing of information in the human brain (Goh et al., 2020), and it has been widely used for sequence learning problems (Graves and Jaitly, 2014; Sutskever et al., 2014). Like the structure of ANN, RNN is also composed of three layers: the input layer, the hidden layer, and the output layer, as illustrated in Fig. 1. The biggest difference from ANN is that RNN has recurrent connections, which means it can capture historical information on what has been calculated in all previous time steps. In other words, the output in RNN depends on the previous computations to some extent.

In classical ANN, the nodes between the layers are interconnected, but the nodes in each layer are independent of each other. In RNN, the nodes in the hidden layer are interconnected, and the nodes of each hidden layer receive the information transmitted by the input layer at current time step *(t)* and the information transmitted by the hidden layer at last time step *(t-1)* simultaneously (Fig. 2). In this way, the recurrent connections in RNN successfully pass previous information to current calculation progress. Therefore, the output value *y* at the current time step *(t)* can be calculated as follows (Fan et al., 2014; Yang et al., 2019):

$$h_t = \phi(W_{xh}x_t + W_{hh}h_{t-1} + b_h) \tag{1}$$

$$y_t = \varphi(W_{hy}h_t + b_y) \tag{2}$$

where x_t and y_t are the input and output values respectively; h_t and h_{t-1} are the hidden state values at current time step *t* and last time step *t-1* respectively; when time step *t* is 0, h_{t-1} becomes h_{-1}, which is required to calculate the first hidden state, and it is typically initialized to all zeroes; W_{xh} is the weight matrix between input and hidden vectors; W_{hh} denotes the weight matrix between different time steps of the hidden vectors; W_{hy} is the weight matrix connecting the hidden information to the output values; b_h and b_y are the corresponding bias vectors of W_{hh} and W_{hy}, respectively; ϕ is the nonlinear activation function of hidden state and is usually a sigmoid function or hyperbolic tangent function; and φ is the nonlinear activation function of input and output vectors, and is usually a sigmoid function or softmax function.

Differing from a traditional deep neural network, the parameters (W_{xh}, W_{hh}, and W_{hy}) used in RNN are unchangeable and shared with all-time steps. This greatly reduces the total number of learning parameters and computational costs. The primary feature of RNN is its hidden state, which captures computed information of previous time steps. Because of this special property, RNN is also used for regression tasks, especially the time-series analysis problems (Kong et al., 2017).

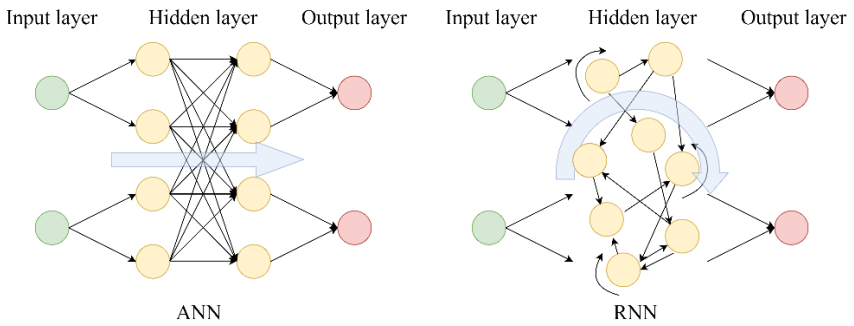


Figure 1. Difference between artificial neural network (ANN) and recurrent neural network (RNN).

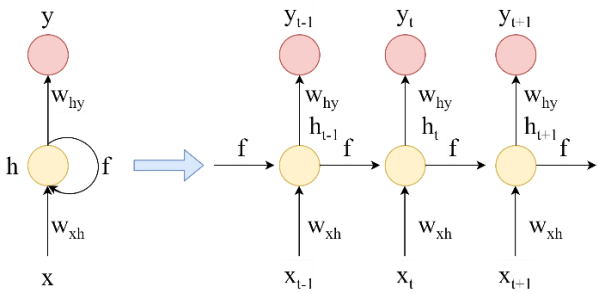


Figure 2. Expanded structure of RNN.

Long Short-term Memory Neural Network

In theory, RNN can make full use of processed information for sequential problems, but in practice it is limited to a few previous time steps due to the problems of gradient vanishing or exploding (Bengio et al., 1994; Hochreiter et al., 2001). Gradient vanishing in RNN refers to the situations where the norm of the gradient for long-term elements drops exponentially to zero, limiting the model capability to learn long-term temporal correlations, while the gradient exploding refers to the opposite problems (Kong et al., 2017). Therefore, conventional RNN is not very applicable for complex sequence learning problems, because the more network layers there are, the more unstable the model will be. To handle these problems, the long short-term memory (LSTM) was proposed by Hochreiter and Schmidhuber (1997), where the biggest improvement is that LSTM has a more complex memory cell, as illustrated in Fig. 3.

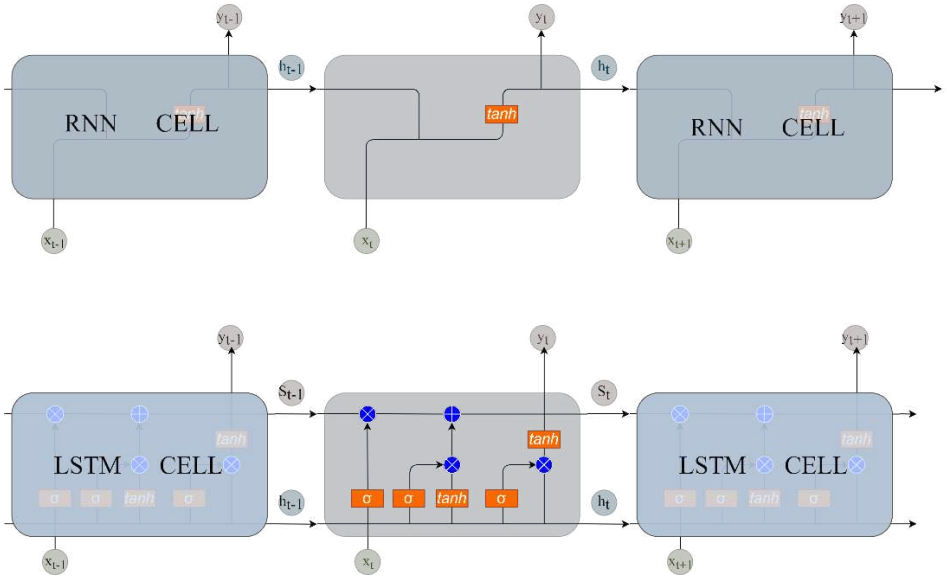


Figure 3. Structure comparison between RNN and LSTM.

The memory cell in LSTM contains three gates: "input gate", "forget gate", and "output gate" (Gers and Schmidhuber, 2000). A detailed review of this design has been reported by many works (Sak et al., 2014; Xu and Niu, 2018; Yang et al., 2019; Jiang et al., 2020), and this work will use a similar example to briefly introduce the concept of LSTM. Assume that the LSTM model has an input sequence $x = (x_1, x_2, \ldots, x_T)$, where x_t denotes the real values at the time step *t*. When x_t is passed into the memory cell, it will be combined with the interaction of the memory cell state s_{t-1} and the intermediate output h_{t-1} to determine which elements of the internal state vector should be updated, maintained, or deleted based on previous information and input values at a current time step. In addition to the internal state, the LSTM structure also controls the data flow into and out of the memory cell by input node g_t, input gate i_t, forget gate f_t, and output gate o_t. A complete LSTM cell can be expressed as follows (Kong et al., 2017):

$$f_t = \sigma(W_{fx}x_t + W_{fh}h_{t-1} + b_f) \tag{3}$$

$$i_t = \sigma(W_{ix}x_t + W_{ih}h_{t-1} + b_i) \tag{4}$$

$$g_t = \gamma(W_{gx}x_t + W_{gh}h_{t-1} + b_g) \tag{5}$$

$$o_t = \sigma(W_{ox}x_t + W_{oh}h_{t-1} + b_o) \tag{6}$$

$$s_t = g_t \Theta i_t + s_{t-1} \Theta f_t \tag{7}$$

$$h_t = \gamma(s_t) \Theta o_t \tag{8}$$

where W denotes the weight matrices for the corresponding inputs of the network activation functions, Θ means an element-wise multiplication, σ is the sigmoid activation function, and γ represents the tanh function. The common initialization of previous information h_t and s_t is zero initialization, i.e., $h_0 = 0$ and $s_0 = 0$.

The memory cell is the most important feature of the LSTM structure, and it can more efficiently use previous information than RNN. The three specially designed gates depend on the current input x_t and the previous output h_{t-1}. The input gate controls how much new information can be passed into the cell, while the forget gate calculates what information will be erased from the previous state. Ultimately, the output gate determines what calculated information at the current time step should be passed. This process continues throughout the whole life cycle before the final results are obtained.

Prophet Model

Prophet is an open-source algorithm developed by Facebook (Taylor and Letham, 2018), and it has been used for time-series analysis based on an additive model (Zunic et al., 2020). It decomposes the time-series data into three main components: trend, seasonality, and holiday (Yan et al., 2019). The governing equation of this model can be expressed as follows (Taylor and Letham, 2018):

$$y_t = g(t) + s(t) + h(t) + \varepsilon_t \tag{9}$$

where $g(t)$ is the trend function that reflects the long-term component in the original data, $s(t)$ denotes the periodic component which has a close relationship with time effect (e.g., yearly, monthly, weekly, and daily seasonality), $h(t)$ represents the violent changes of holidays that occur irregularly, and ε_t is the error term which is assumed to be normally distributed.

The long-term trend is the most important component of the landslide displacement, and it is mainly controlled by internal factors, e.g., geologic conditions and material properties. There are two trend models implemented in Prophet: a saturating growth model and a piecewise model. Considering similar step-wise characteristics of the landslide displacement in this work, the piecewise model was adopted to model the long-term trend, and it can be expressed as follows:

$$g(t) = \frac{C(t)}{1+exp(-(k+a(t)^T\delta)(t-(m+a(t)^T\gamma)))} \tag{10}$$

where $C(t)$ is the carrying capacity of the system at any time point, $k + \alpha(t)^T\delta$ is the time-varying growth rate, δ denotes the rate adjustments, m is the offset parameters, and γ is set as correct adjustments to make the function continuous.

Due to the significant effects of external factors such as seasonal rainfall and the periodical fluctuation of the reservoir water level, the landslide displacement usually shows a similar development pattern, that is, periodicity (Zhang et al., 2020a). To fit and forecast these effects, the seasonality function should contain periodic functions of time. Prophet uses a Fourier series which provides a flexible model. The seasonal effects $s(t)$ can be expressed as follows:

$$s(t) = \sum_{n=1}^{N}(a_n\, cos(\frac{2\pi nt}{P}) + b_n\, sin(\frac{2\pi nt}{P})) \tag{11}$$

where P is a regular period which is expected as a feature of the time-series data (e.g., $P = 365$ for yearly data or $P = 7$ for weekly data) and N is the number of cycles.

For commercial purposes, the holiday effects are considered in Prophet to model and forecast unusual changes on holidays or some big events. There is no such effect on the landslide displacement, so it is not considered in this work.

MARS Algorithm

Multivariate adaptive regression splines (MARS), first proposed by Friedman (1991), is a flexible procedure which models complex relationships that are nearly additive or involve interactions with fewer variables. It is a non-parametric regression technique based on a divide-and-conquer strategy, partitioning the training data sets into separate piecewise segments (splines) with different gradients, each of which is fit with its own regression equation as the "knot" points are crossed (Lee and Chen, 2005; Zhou and Leung, 2007). With this special attribute, this methodology excels at capturing both linear and nonlinear relationships that often hide in high-dimensional data, and hence can efficiently reveal complex data patterns and handle multivariate problems. Similarly, these problems are also common in the geotechnical engineering field, indicating the method's wide potential for application (Zhang and Goh, 2013; Zhang and Goh, 2016; Zhang et al., 2020c).

The general MARS function can be presented as follows:

$$f(x) = a_0 + \sum_{m=1}^{M} a_m \prod_{k=1}^{K_m}[s_{km}(x_{v(k,m)} - t_{km})]_+ \tag{12}$$

where a_0 and a_m are parameters; M denotes the number of piecewise curves, also known as basis functions; s_{km} takes the value of 1 or -1 and indicates the right or left sense of the associated step function; $v_{(k,m)}$ denotes the label of the independent variable; and t_{km} is the knot location.

The optimal MARS model is built in two stages: a forward stepwise selection process and a backward "pruning" process. Firstly, many basis functions are constructed to fit the data, and this process continues until the model reaches the maximum model size that is predetermined. However, this model usually suffers from the issue of overfitting, which means it has a high accuracy fit to the data used for developing this model but will not perform well with the new data. Then the backward "pruning" process is applied to build this model with better generalization ability by deleting the basis functions that contribute least to the model fitting. At this stage, the generalized cross-validation (GCV) criterion is used to compare the variable importance when it is removed from the model.

Support Vector Machine Model

The support vector machine (SVM) was first proposed for the classification problems (Cortes and Vapnik, 1995), and has been extended to the realm of regression problems, which is called the support vector regression (SVR). For a given set of l training samples $\{((x_1, y_1), \ldots, (x_l, y_l))\}$, $x_i \in \mathbb{R}^d$ means the i_{th} input pattern from the d dimension input space and has a corresponding target value $y_i \in \mathbb{R}$ for $i = 1, \ldots, l$, where R is the set of real number. The goal of this method is to find a function that approximates mapping from an input domain to target values based on a training set and has a minimum generalization error. The general form of this function can be expressed as follows (Zhou and Leung, 2007):

$$f(x) = w \cdot \phi(x) + b \tag{13}$$

where $w \in R^n$ and denotes the weight vector, $b \in R$ and is bias, $\cdot$ represents the dot product in R^n, and ϕ is a non-linear transformation from $R^d$to a higher dimension space R^n (i.e., $n > d$).

Assuming that the transformation ϕ is unknown, the kernel functions can be constructed to enable the dot product to be performed in a high-dimensional feature space using the original data in a low-dimensional space. Commonly-used kernel functions include the linear, polynomial, and radial basis function (RBF) (Smola and Schölkopf, 2004). When using this method for solving regression problems, the model performance is closely related to the kernel function, the penalty parameter, and the radius factor.

Model Development

The Displacement Model

The landslide displacement is greatly affected by both internal and external factors, and its development can be decomposed into two components: a long-term trend and a periodic term based on specific influences. The internal factors, such as geological conditions and material properties, mainly control the landslide displacement and make it grow approximately monotonically with time at a long-time scale. The external factors mainly contain rainfall and the reservoir water level, and they have the lagging effect on the landslide displacement, which makes surficial deformation vary periodically. The accumulated displacement can be considered as a sum of these two components as follows:

$$s(t) = f(t) + g(t) \tag{14}$$

where $s(t)$ is the total displacement recorded by monitoring systems, $f(t)$ denotes the long-term trend displacement, $g(t)$ is the periodic displacement, and t is time. Clearly, sudden actions (i.e., earthquakes and mine explosions) can pose a serious threat to the landslide stability and can cause rapid change within hours. However, given the existing monitoring tools and methods, the abrupt displacement caused by such random factors cannot be predicted. Due to the difficulty and uncertainty, such a scenario was not taken into consideration in this work.

The prediction Process

Four machine learning methods were used in this work to predict the landslide displacement. The two displacement components (the trend term and the periodic term) were predicted separately via a mathematical function and machine learning methods (LSTM, MARS, and SVM), as shown in Fig. 4. Due to the similar mechanism of the Prophet model and the proposed model in this work, we use the former directly to predict the total displacement, which works more efficiently.

Thus, the prediction process can be implemented as follows:

1. The monitored total displacement should be decomposed into two components.

2. The trend displacement is time-dependent, and it increases steadily over time, which can be fitted with a polynomial function with high accuracy.

3. The periodic displacement is closely affected by rainfall and reservoir water level, and its fluctuation with time is more complex. By analyzing the correlation between rainfall, reservoir water level, and displacement, several controlling variables (seen in Section 4.3.1) were determined to predict the Bazimen landslide in the Three Gorges Reservoir area, using the mentioned methods to predict the periodic displacements, as illustrated in Fig. 4. In this part, the one-step forecasting method was used to predict periodic displacement at the next time step. In general, this method performs well for forecasting time-series data when prediction accuracy is required. Then, the total displacement can be obtained by adding the predicted trend and the periodic displacement.

4. At the same stage, the total displacement can be predicted directly with the Prophet model, completely using the recorded accumulated displacement. This prediction model does not require complex data processing and relationship consideration; it is much easier to be implemented. In this case, Prophet was used to predict a multi-step displacement time series. The biggest difference from the one-step method is that this one can predict data for more time steps. This may be very helpful when decision-makers need more predicted time points to act, with a longer-term view.

5. Finally, the predicted total displacements obtained by different machine learning methods were compared with the monitored dataset to determine the best model performance.

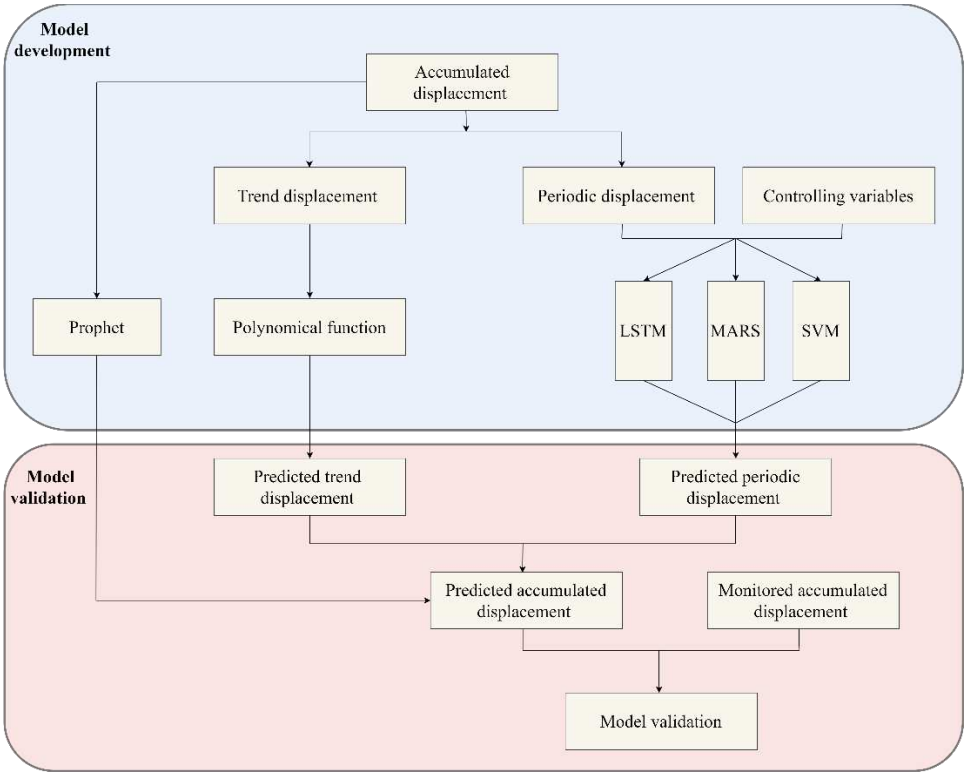


Figure 4. Flowchart of the displacement prediction process.

The entire dataset contains 175 monitoring points, which were recorded monthly from Jun. 2004 to Dec. 2018. In addition to the dataset of the year 2018 for testing, the remaining dataset was divided into two components: one for training (80%) and the other for validation (20%).

Evaluation of Modeling Performance

Three common statistical criteria, including the mean absolute error (MAE), the root mean square error (RMSE), and the coefficient of determination (R^2), are used here to evaluate the performance of these models. MAE is defined as follows:

$$MAE = \frac{1}{m}\sum_{i=1}^{m}|y_i - \hat{y}_i| \qquad (15)$$

where m is the number of samples, y_i is the observed value of i_{th} sample, and $\hat{y}_i$ denotes the predicted value on the same sample i_{th}.

The RMSE is a scale-dependent measure, and it is efficient for comparing different methods applied to one same dataset. The definition of this criteria can be expressed as follows:

$$RMSE = \sqrt{\frac{1}{m}\sum_{i=1}^{m}(y_i - \hat{y}_i)^2} \qquad (16)$$

Notations used in Eq. 16 are the same as those shown in Eq. 15. The lower the value of RMSE or MAE, the stronger the forecasting capacity of the model.

The R^2, defined by Eq. 17, is the square of the Pearson correlation coefficient (ρ) and it is usually used to evaluate the fitting quality of a model on data. It ranges from 0 to 1, with a higher value indicating a stronger correlation.

$$R^2 = \left[\frac{\sum_{i=1}^{m}(y_i-\overline{y})(\widehat{y_i}-\tilde{y})}{\sqrt[2]{\sum_{i=1}^{m}(y_i-\overline{y})^2}\sqrt[2]{\sum_{i=1}^{m}(\widehat{y_i}-\tilde{y})^2}} \right]^2 \qquad (17)$$

where $\tilde{y}$ is the average of predicted results, $\overline{y}$ denotes the mean of real values, and other notations are as same as in Eqs. 15 and 16.

CASE STUDY

Background Information

The Bazimen landslide is located in Guizhou Village of Zigui County, on the right bank of the Xiangxi River (30°58′16″N, 110°45′30″E), which is a major tributary of the Yangtze River. It is approximately 0.8 km upstream of the estuary where the Xiangxi River meets the Yangtze River and 38 km from the Three Gorges Dam (Fig. 5). The slope angle ranges from 10° to 30°, with an initial sliding direction orientated at N120°. The upper boundary of the landslide is at the interface between bedrock and soil. The left and right boundaries are both defined by homologous gullies. The landslide is currently at an elevation of 139-280 m, and the original elevation of the front part was at 55 m before the first impoundment of the TGR in 2003. The landslide is fan-shaped, and the sliding body is gentle at the lower part while steep at the higher part. It covers an area of approximately 1.35×105 m^2, with a longitudinal dimension of 380 m and a width of 100-350 m, and has an estimated volume of 2.0×106 m^3.

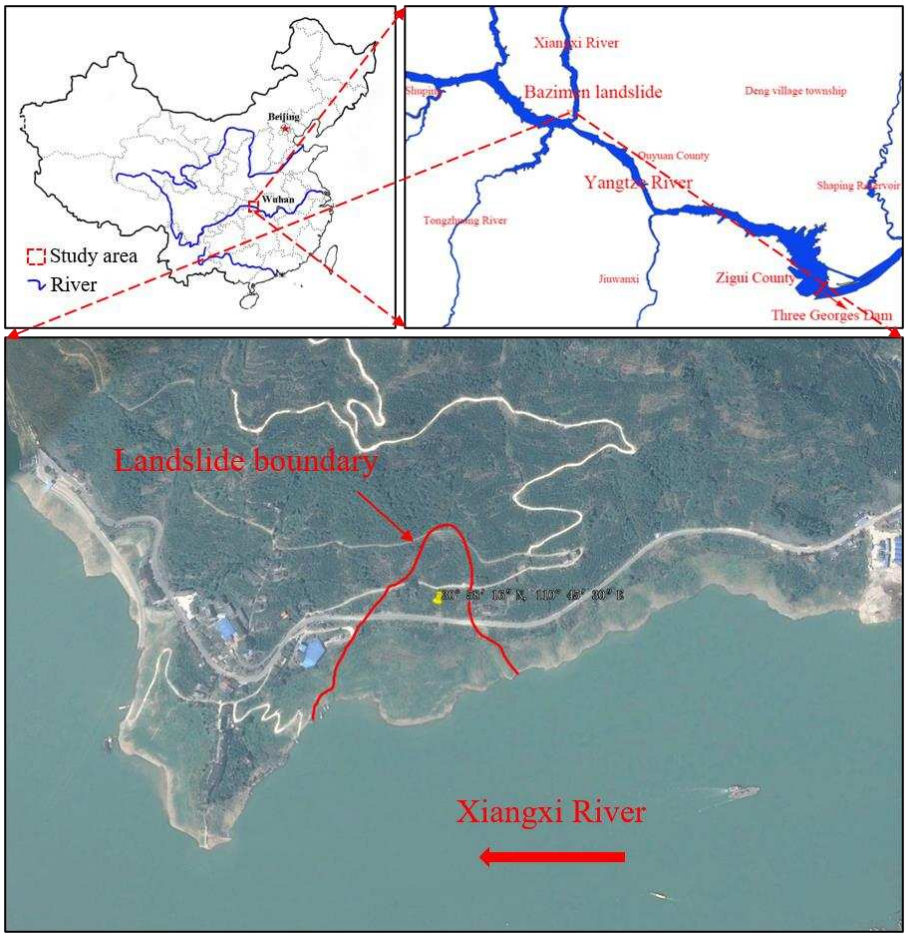


Figure 5. Location and the satellite map of the Bazimen landslide in the Three Gorges Reservoir area.

The sliding masses of the Bazimen landslide are primarily composed of sandy shale, sandstone, gravel, and clay. Based on the borehole data, there are two main sliding surfaces found (Du et al., 2013; Yang et al., 2019). The deeper one is the initial sliding surface at a depth of 10 to 35 m, and the shallower one is the secondary sliding surface with a depth of 6 to 18 m. The materials of these two sliding surfaces are both silt and clay with fragmented rubble. The thickness of the sliding zone is thick in the middle area and thin at the upper and lower part, as shown in Fig. 6.

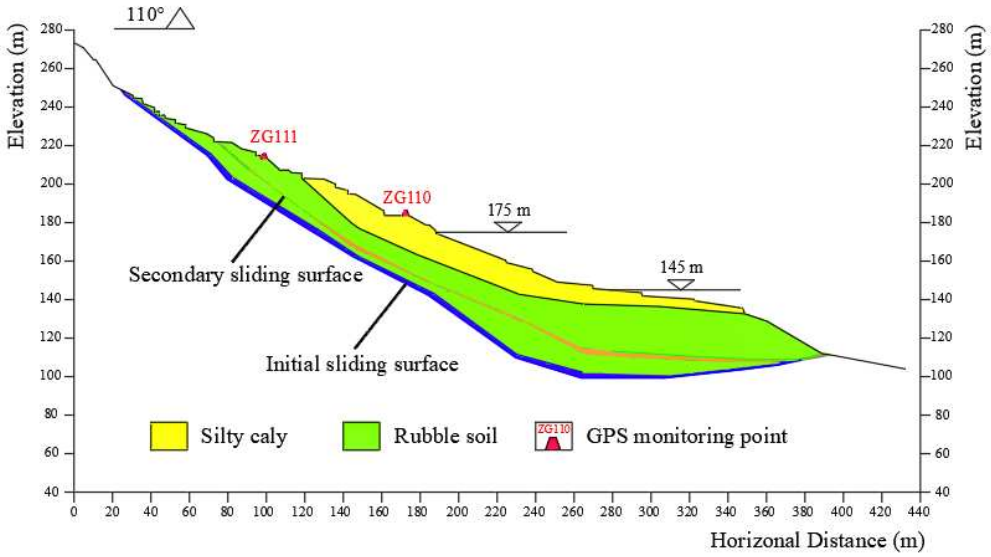


Figure 6. Schematic geological cross-section I-I' of the Bazimen landslide (modified from Zhang et al. (2020a)).

Analysis of the Monitoring Data

Currently, there are 10 GPS monitoring points installed on the landslide, and the numbered stations ZG110 and ZG111 have been recording data since July 2003. Fig. 7 shows the data of the accumulated displacement, rainfall, and reservoir water level from 2003 to 2018. It can be observed that the displacement in the upper part of the landslide (monitored by ZG111) increased faster than that in the middle part (monitored by ZG110). The displacement characteristics of the landslide indicate that the development model is “advancing”; the landslide started from the upper part and developed downwards with increasing displacement. Compared with the monitored data of ZG110, the data recorded at ZG111 has more obvious piecewise characteristics, which means it can better help to explore the potential relationship between landslide displacements and external triggering factors. It is therefore used to establish the forecasting model.

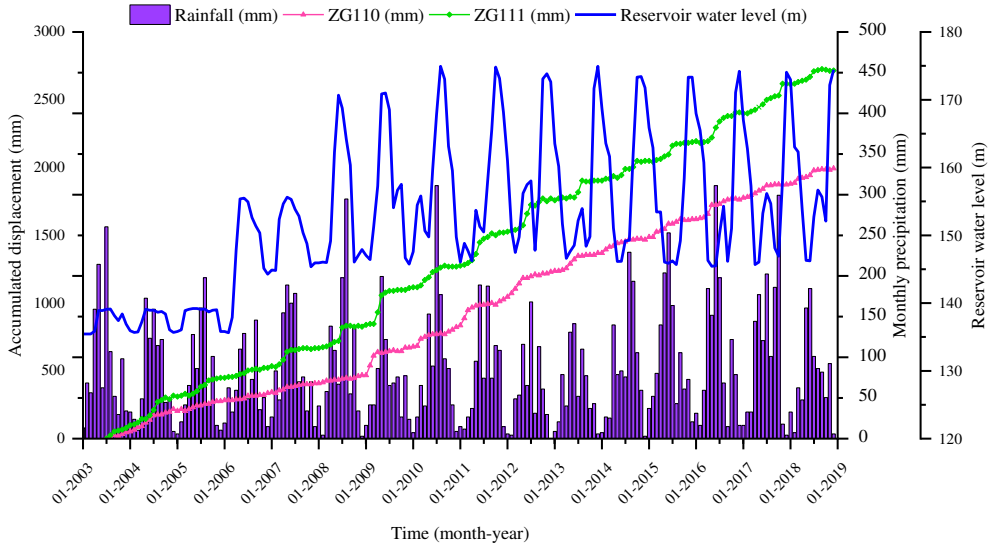


Figure 7. The accumulated displacement, rainfall, and reservoir water level at Bazimen landslide.

The displacement characteristics related to controlling factors can be analyzed and summarized as follows:

1. There is a close correspondence between the scheduling of the reservoir and the accumulated displacement of the landslide: the displacement was kept almost unchanged when the reservoir water level increased or operated steadily; it grew intensely during the period reservoir drawdown. Every time the reservoir water level dropped, the accumulated displacement rose. The reservoir water level varied annually from 2007 to 2018, and the accumulated displacement increased correspondingly within that time. However, the displacement did not respond immediately to the decline in the water level. Fig. 7 suggests that the water level exerted a lagging effect on the accumulated displacement, and the latter always began to increase after the former decreased for one or two months.

2. Rainfall also affects the stability of landslide, though the accumulated displacement may be weakly correlated with this factor (Zhang et al., 2020a). As shown in Fig. 7, the accumulated displacement grew rapidly during the rainy season, during which heavy rainfall occurs. Although the reservoir water level starts rising in late August each year, high-intensity rainfall may relent to some extent, while the landslide displacement still continues to increase in this period, indicating that rainfall plays a certain role in promoting the landslide displacement.

3. The landslide deforms sharply under the coupling effect of rainfall and reservoir drawdown, and the monitored displacements have obvious step-wise characteristics, indicating the influence of periodic factors. Moreover, the deformation rate of the landslide increases suddenly and the accumulated displacement curve shows a steep jump during the flood season, from May to August, when the maximum precipitation occurs and the reservoir water level decreases at the fastest drawdown velocity. It can be inferred that during the drawdown period of the reservoir water level, superimposed rainfall conditions will further aggravate the landslide displacement, which is more unfavorable to the stability of the landslide.

DATA PROCESSING AND RESULTS ANALYSIS

Displacement Decomposition

As mentioned in section 2.2, the accumulated displacement mainly contains two components: the long-term trend and the periodic terms. After removing the trend term from the total displacement, the residue is the periodic displacement. Many studies have shown that the moving average method is applicable for the displacement decomposition (Du et al., 2013; Yang et al., 2019), and it can be used to calculate the trend displacement as follows:

$$f(t) = \frac{y_t + y_{t-1} + \ldots + y_{t-k+1}}{k} (t = k, k+1, \ldots, N) \tag{18}$$

where $f(t)$ is the trend term at time t; y_t is the accumulated displacement at time t; k is the moving average cycle, was set as 6 months here since the rainy and dry seasons each last almost half a year ; and N is the total number of samples.

Prediction of Trend Displacement

The trend displacement shows a stable development model with time (Fig. 8), and it is usually fitted with a nonlinear regression model (Xu and Niu, 2018). In this work, both a linear and a cubic function were developed and compared to fit the long-term trend curve. This process was conducted using the polynomial regression model in the Scikit-learn package, backend with TensorFlow 2.0. The R^2 of a linear regression model for this dataset is 0.9956, while that of a cubic model is 0.9974, indicating that the latter one performs slightly better. The predicted values and the monitored data of the trend term are shown in Fig. 9, and the fitting function works well with a polynomial form, as illustrated in Eq. 19.

$$f(t) = -0.0003t^3 + 0.0844t^2 + 8.7555t + 174.7 \tag{19}$$

where $f(t)$ is the predicted value of the trend term at time t.

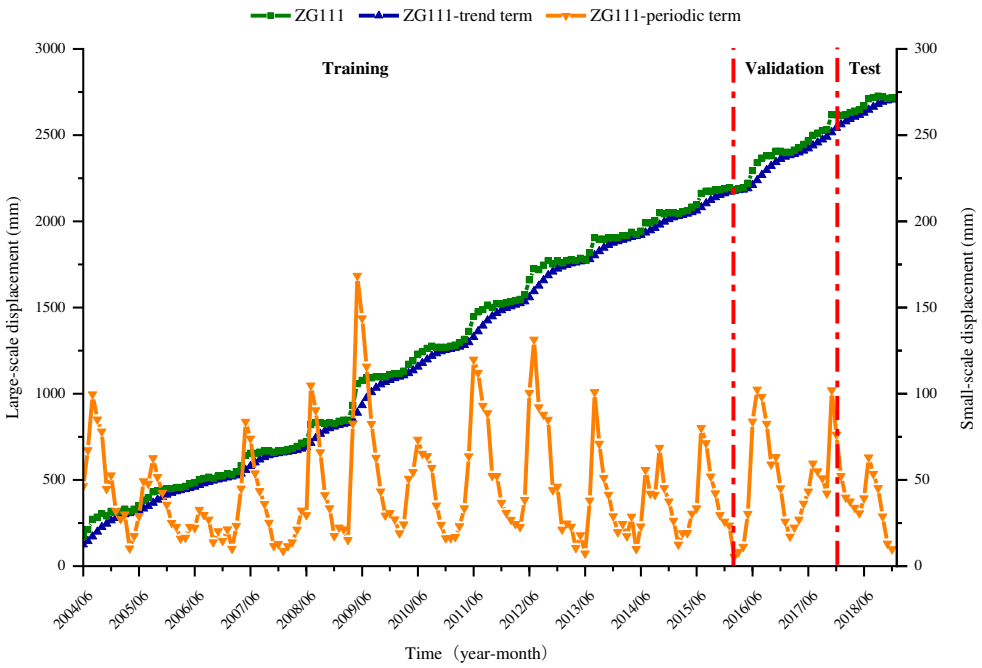


Figure 8. Decomposition results of the accumulated displacement monitored at the ZG111 station.

Prediction of Periodic Displacement

Controlling Factors

The model performance on the data is primarily evaluated by the accuracy, and it is thus of great importance to explore the functional relationships between the input variables and the target values. As analyzed, the coupling effect of seasonal rainfall and annual fluctuation of the reservoir water level plays an important role in triggering landslide deformation. Therefore, like common regression methods, the controlling factors (i.e., rainfall and reservoir water level) were used as input sequences and the periodic displacement was taken as the output value in this work.

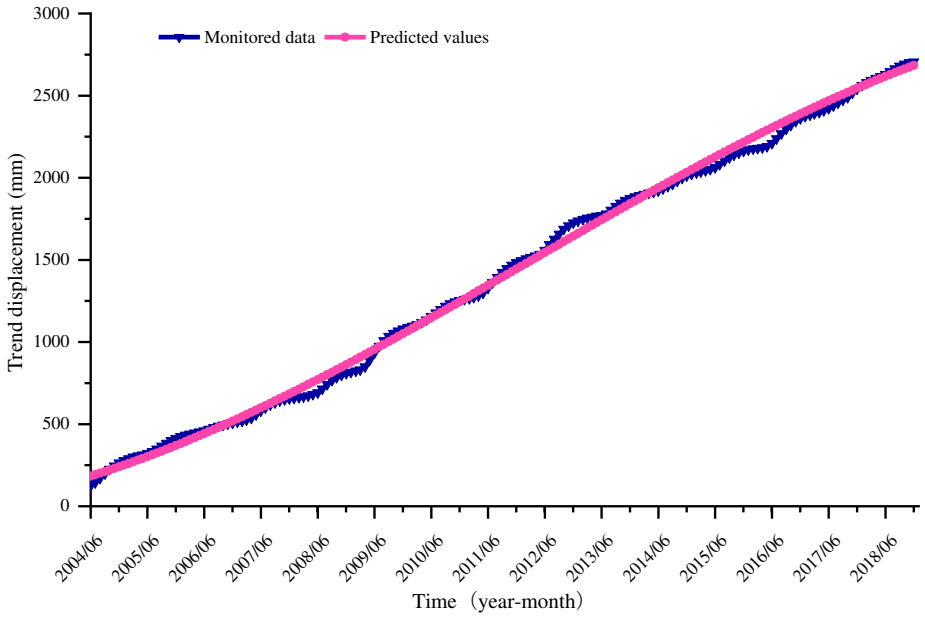


Figure 9. Monitored and predicted trend displacement at ZG111 of the Bazimen landslide.

In addition to the external controlling factors, the deformation state at different evolutionary stages also affects the prediction accuracy. As reported by Du et al. (2013), the performance of influencing factors depends on whether the slope is stable or not. This means even important triggering factors may not impose significant threats in terms of slope displacements when the slope is under stable conditions. In contrast, under extremely unstable conditions, even a slight disturbance can cause landslides to deform dramatically. Therefore, the stability state should be given precedence when considering influences on landslide displacement. This can be revealed by previous data, and some studies have also shown the necessity and efficiency of a concerned model when considering this factor.

The candidate variables are shown in Table 1, defined as v_i, where v means variable and i means the number. The Pearson's correlation coefficient *(r)* is also calculated to measure the association strength between input variables and the periodic displacement in Table 1. Finally, considering the r values, v_2, v_3, v_4, v_5, v_7, and v_8 were selected as input variables to build the model.

Table 1. The candidate variables and the calculated Pearson's correlation coefficient.

Input type	Candidate variables	*R*
Precipitation	v_1, the cumulative precipitation at last month	0.484
	v_2, the cumulative precipitation during last 2-month period	0.544
	v_3, the cumulative precipitation during last 3-month period	0.523
Reservoir water level	v_4, the reservoir level at current month	0.187
	v_5, the change of the reservoir level at last month	0.224
	v_6, the decline of the reservoir level at last month	0.155
Deformation state	v_7, the increased displacement over last month	0.755
	v_8, the increased displacement over last 2 months	0.626
	v_9, the increased displacement over last 3 months	0.488

Development for the LSTM Model

The entire dataset was divided into three parts: the data of year 2018 for testing, 80% of the remaining dataset for training, and the last 20% for validation (Fig. 8). Data in the training dataset were used for model construction and the validation dataset was used to verify the prediction capacity. Considering the size of this dataset, which contains 175 data points, test dataset was also used in this work to check the model's generalization ability. In some cases, when the dataset only has a small number of data points, the interpolation method may be helpful, and the test dataset can be omitted. The model constriction was implemented with TensorFlow 2.0 in the Python environment.

As aforementioned, the LSTM model is very sensitive to the data structure, and the normalization will avoid convergence problems to some extent. Therefore, both the input variables and the target values were normalized to [-1, 1]. The grid search method was used to optimize the model, as it can achieve a balance between the model accuracy and computational time. The process of this method can be expressed as follows: reasonable values of each parameter are combined via the cross-validation method in the training set, and then the best parameter combination can be automatically determined. In essence, it is a kind of traversing method, and it may be time-consuming to determine the optimal combination of parameters, depending on the complexity of models. Considering the scale of the dataset, a four-layer LSTM model was developed, with the first three layers as LSTM layers and the last layer as a dense layer.

The LSTM model uses previous data (selected variables as input sequences) to build potential relationships for forecasting target values, and the time step is an important parameter to be considered, which shows how many time steps of previous data are considered for forecast. The grid search method shows that the optimal time step is 3 in this work, which means the latest data are more useful to build the LSTM model. The gird search method was also used for optimizing parameters of other three machine learning methods mentioned in this work: MARS, SVM, and Prophet.

Predicted Periodic Displacement

The predicted and monitored periodic displacements at the ZG111 observation station are shown in Fig. 10, where the training and validation dataset using the MARS, SVM, and LSTM models are presented separately. The comparisons between the evaluation criteria of the datasets and models are illustrated in Table 2. It can be observed that the LSTM model performed well in both training and validation datasets. The RMSE and MAE values were 8.79 and 6.34 mm in the training dataset and

were 8.72 and 6.02 mm in the validation dataset, respectively. Compared with other models, the LSTM model shows a better forecasting capacity and the results indicate that this dynamic model can capture the complex relationships between input variables and target values. In terms of the SVM model, a comparison between the results obtained by different kernel functions shows that the SVM model with a RBF kernel has better prediction capacity. Therefore, the SVM model with the RBF kernel function was used as a representative of SVM models for later analysis. Compared with the SVM model, the MARS model has a similar forecasting performance on the two datasets, with close evaluation criteria and predicted values.

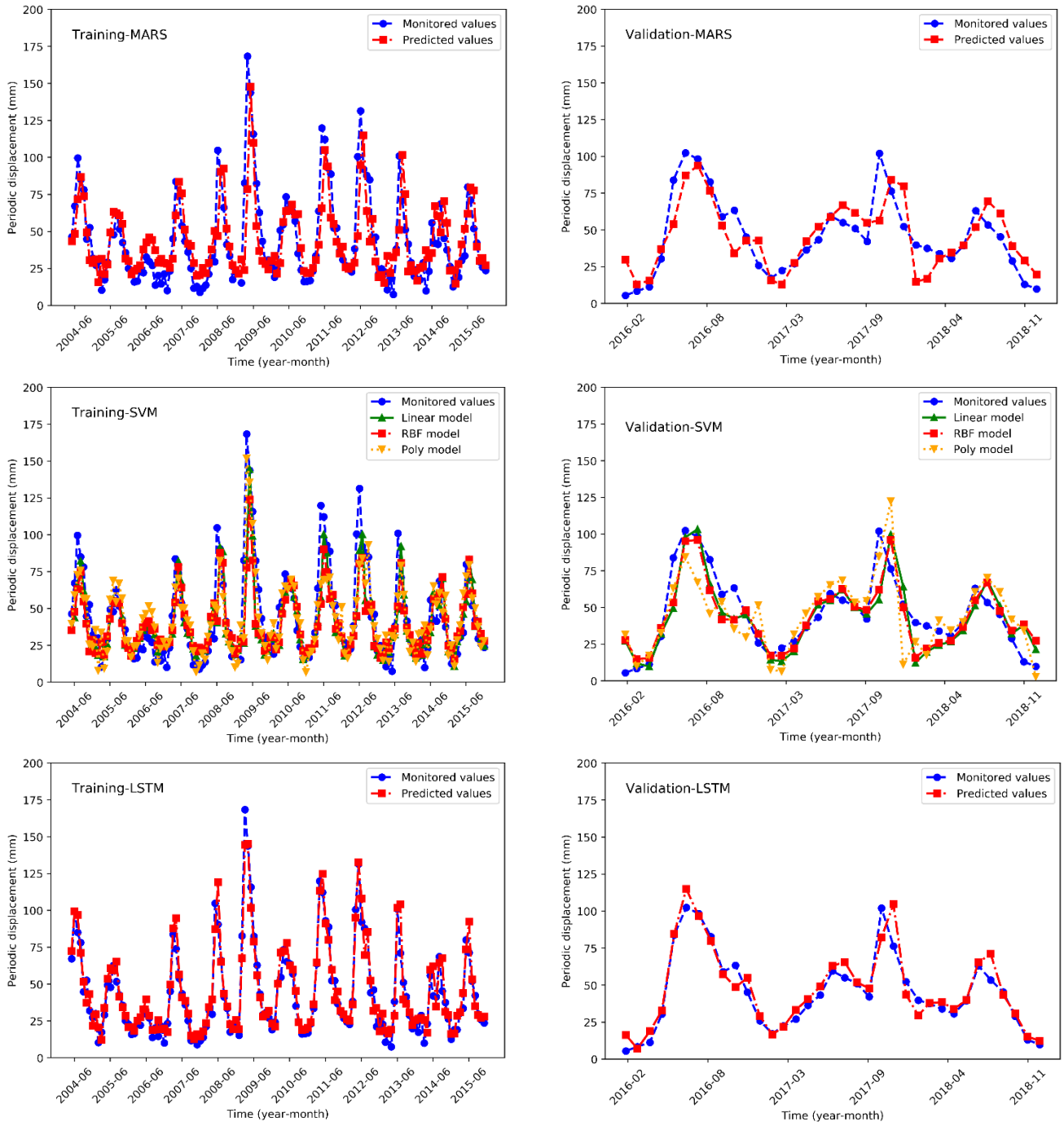


Figure 10. Predicted and monitored periodic displacements at ZG111 with the MARS, SVM, and LSTM models.

Table 2. Comparison of evaluation criteria for periodic displacements with the MARS, SVM, and LSTM models.

Models	Training Dataset		Validation Dataset	
	RMSE (mm)	MAE (mm)	RMSE (mm)	MAE (mm)
MARS	19.11	13.38	15.79	12.16
SVM (RBF)	19.73	13.47	14.40	10.76
LSTM	8.79	6.34	8.72	6.02

In general, the displacements predicted by the MARS and SVM methods are basically consistent with the monitored values, except the local peak and irregular displacements. For example, for periodic displacements during November 2016, October 2017, and August 2018, the predicted values by the two models differ significantly from monitored values. This indicates that the prediction capacity of a static model can be seriously affected when external triggering factors (i.e., rainfall and reservoir water level) change rapidly. Although the LSTM has good forecasting capacity overall, this phenomenon is also particularly obvious for this model, which uses previous information to predict target values at the current time step. When a local peak or an irregular displacement occurs, this model still uses what it has learned from the conventional and regular data, which may cause large errors. Furthermore, the peak displacements always occur during the flood season, when the coupling effect of high-intensity rainfall and the rapid change of the reservoir water level is stronger. It is therefore notable that a model's prediction performance on irregular and unconventional data should be examined in future work.

Predicted Accumulated Displacement

As mentioned in Section 2.2, for the MARS, SVM, and LSTM models, the predicted accumulated displacement should be the sum of the predicted trend and periodic displacements. The trend displacement can be obtained by Eq. 19, which was fit based on historical displacements. For the Prophet model, due to the similarity of its mechanism and the proposed model of this work, the former was used directly to predict the total displacements based on recorded values. This model does not require the process of displacement decomposition, nor does it need previous data of a specific prior time step to predict displacements of multiple time steps.

Contrary to the other three methods that attempt to find relationships between landslide displacements and external triggering factors, the Prophet model tries to capture the time characteristics of displacements. It is thus very convenient and simple for users, as this model does not require finding candidate variables but the displacement itself. Fig. 11 shows the Prophet model predictions for nearly 3-year displacements (February 2016 to December 2018), based on the explored model it has learned from previous data (June 2004 to January 2016). Although the predicted total displacements do not agree well with the monitored data, the step-wise development pattern was well captured by this model. In some sense, it is the real forecasting model, because it predicts based on learned development patterns rather than a simple function of input and output values, and more importantly, this model does not require extra input variables except historical displacements.

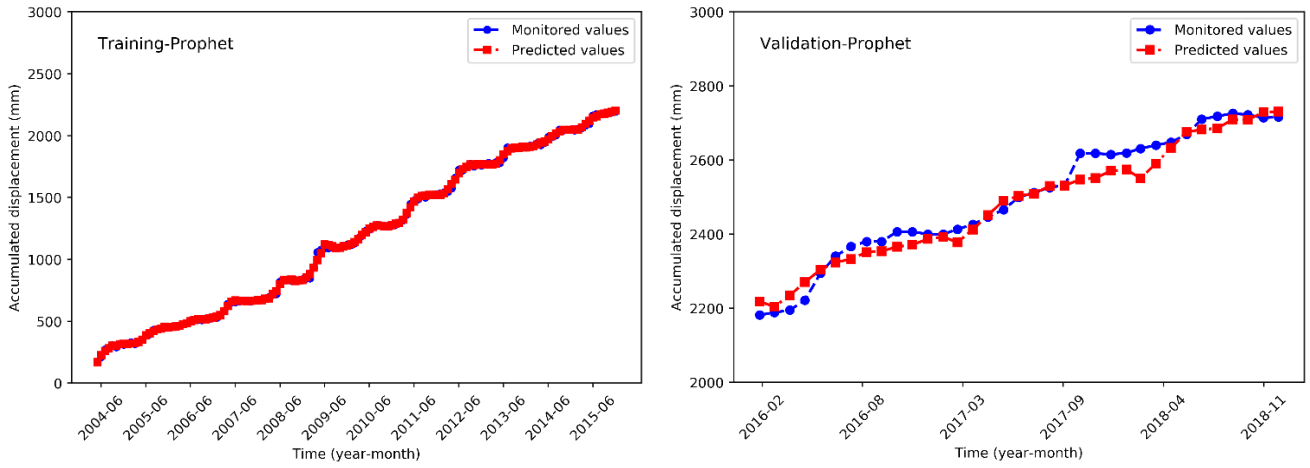


Figure 11. Predicted and monitored accumulated displacements at ZG111 with the Prophet model.

Taking the 2018 displacements as the test dataset, the predicted and monitored values shown in Fig. 12, and the evaluation criteria listed in Table 3, we arrive at the following conclusion. Generally, the LSTM model shows the highest prediction accuracy, the MARS and the SVM models have similar predicted results with medium accuracy, and the Prophet model has relatively poor prediction capacity. The values of the RMSE and MAE with the LSTM model are 18.78 and 17.03 mm respectively, and these values of the Prophet model are 36.37 and 30.09 mm.

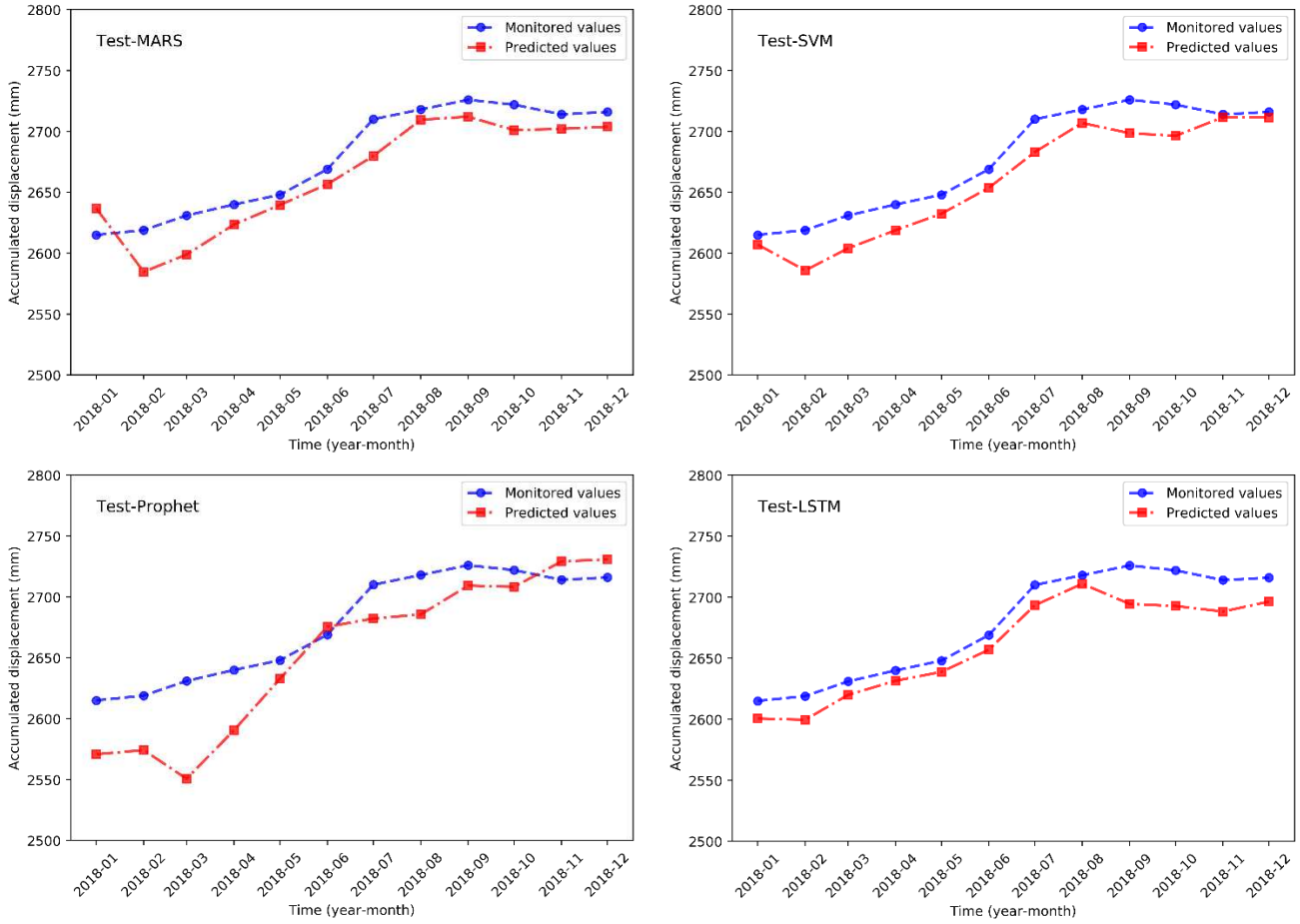


Figure 12. Predicted and monitored accumulated displacements at ZG111 with the MARS, SVM, LSTM, and Prophet

Table 3. Comparison of evaluation criteria for accumulated displacements with the MARS, SVM, and LSTM models.

Models	Test Dataset	
	RMSE (mm)	MAE (mm)
MARS	20.56	18.56
SVM (RBF)	20.62	18.18
LSTM	18.78	17.03
Prophet	36.37	30.09

DISCUSSION

In this work, the LSTM model performs better both in predicting periodic displacements and accumulated displacements with Eq. 19. This model uses an input sequence at a specific length, containing information with a period of history, to predict target values at the current time step. Different from the other three methods mentioned in this work, this model can make full use of historical information, based on the special "gate" design. This also makes it the most time-consuming for building, developing, and testing. The LSTM model build dynamic connections between previous input variables at different time steps

and target values, which means learned experience is continuously utilized and modified for current tasks. During this process, the model can update the potential rules by memorizing useful information and removing invalid rules. In other words, the memory cell of this model makes it possible to better reflect the dynamic evolution process of the landslide.

For the same datasets, the two classical machine learning methods, the SVM and the MARS models, have poorer model performance. The lack of a similar memory cell in the two models may be the most important reason for this. These two models do not build connections between previous data at different time steps and the target values, which means that the models can only use historical information at a specific time point to predict the displacement correspondingly. However, the latest data structures differ from historical ones, and this may lead to errors to some extent. It is therefore suggested by some studies that in order to establish a more accurate and reliable forecasting model, the datasets should be updated timely by removing old data and adding new data (Du et al., 2013; Yang et al., 2019).

In terms of the Prophet model, its performance is inferior to the above three models. However, its advantage does not lie in the accuracy of a short forecasting period. This model implemented the time series analysis automatically and it predicted target values based on the learned trend and seasonal features. Moreover, this model does not require complex data processing and variables selection, which means it is much easier and more convenient to be carried out. In addition, because this model is based on capturing characteristics between time and displacement, it is possible to predict the target values over a longer time period than values at the next time step. It can be reasonably inferred that this model may be very applicable for engineering purposes, where cost control and time management are planned from a longer-term perspective rather than a specific time step.

SUMMARY AND CONCLUSION

In this work, there are four machine learning methods—MARS, SVM, LSTM and Prophet—applied for the slope displacement prediction. The predictive results by these models generally show good consistency with the monitored displacements, which indicates that the proposed model could handle the dynamic and nonlinear relationships between the landslide displacement and external triggering factors, such as seasonal rainfall and periodic fluctuation of the reservoir water level.

Compared with the other three methods, the LSTM model shows a significant potential for dynamic landslide displacement prediction, as it builds connections between historical information and current tasks. The special design of the memory cell may be the main reason for its better performance. Given new inputs, this model can combine the memorized rules and previous information to achieve more accurate predictions. By continuously repeating this process, this model can remove invalid rules and retain useful ones to update learned relationships. In addition, this process continues throughout the entire life cycle of this model.

The SVM and MARS models show a similar forecasting ability, but their deviation is large when external triggering factors become irregular and uncommon. The static mechanisms may account for it. Compared with LSTM, both SVM and MARS try to find relationships between landslide displacement and input triggering factors at a specific time point. These two methods cannot reflect the dynamic responses hidden behind functions.

The Prophet model shows its priority and convenience in predicting displacements with a longer time period, as it can learn relationships between total displacements and time. However, it achieves the ability of predicting multi time steps at the cost of model accuracy. Therefore, it can be useful for cost control and time management problems, which require longer period information for better estimations.

ACKNOWLEDGEMENT

The authors would like to acknowledge the dataset provided by the National Cryosphere Desert Data Center. (http://www.ncdc.ac.cn). In addition, the authors are grateful for the financial support from the National Key R&D Program of China (Project No. 2019YFC1509605), and the High-end Foreign Expert Introduction Program (No. G20200022005) as well as the Science and Technology Research Program of the Chongqing Municipal Education Commission (No. KJZD-K201900102).



REFERENCES

Bengio, Y., Simard, P., and Frasconi, P. (1994). "Learning long-term dependencies with gradient descent is difficult." *IEEE transactions on neural networks*, 5, 157-166.

Cao, Y., Yin, K., Alexander, D.E., and Zhou, C. (2016). "Using an extreme learning machine to predict the displacement of step-like landslides in relation to controlling factors." *Landslides*, 13, 725-736.

Chen, L., Zhang, W., Zheng, Y., Gu, D., and Wang, L. (2020). "Stability analysis and design charts for over-dip rock slope against bi-planar sliding." *Engineering Geology*, 275, 105732.

Cortes, C., and Vapnik, V. (1995). "Support-vector networks." *Machine learning*, 20, 273-297.

Du, J., Yin, K., and Lacasse, S. (2013). "Displacement prediction in colluvial landslides, three Gorges reservoir, China." *Landslides,* 10, 203-218.

Fan, Y., Qian, Y., Xie, F.-L., and Soong, F.K. (2014). *TTS synthesis with bidirectional LSTM based recurrent neural networks*, Interspeech.

Friedman, J.H. (1991). "Multivariate adaptive regression splines." *The annals of statistics*, 1-67.

Gers, F.A., and Schmidhuber, J. (2000)." Recurrent nets that time and count." *IEEE*, 189-194.

Goh, A.T.C., Zhang, R.H., Wang, W., Wang, L., Liu, H.L., and Zhang, W.G. (2020). "Numerical study of the effects of groundwater drawdown on ground settlement for excavation in residual soils." *Acta Geotechnica,* 15, 1259-1272.

Graves, A., and Jaitly, N. (2014). *Towards end-to-end speech recognition with recurrent neural networks*, 1764-1772.

Hochreiter, S., Bengio, Y., Frasconi, P., and Schmidhuber, J. (2001). "Gradient flow in recurrent nets: the difficulty of learning long-term dependencies, A field guide to dynamical recurrent neural networks." *IEEE Press*.

Hochreiter, S., and Schmidhuber, J. (1997). "Long short-term memory." *Neural computation*, 9, 1735-1780.

Huang, F., Huang, J., Jiang, S., and Zhou, C. (2017). "Landslide displacement prediction based on multivariate chaotic model and extreme learning machine." *Engineering Geology*, 218, 173-186.

Jian, W., Xu, Q., Yang, H., and Wang, F. (2014). "Mechanism and failure process of Qianjiangping landslide in the Three Gorges Reservoir, China." *Environmental Earth Sciences.* 72, 2999-3013.

Jiang, H., Li, Y., Zhou, C., Hong, H., Glade, T., and Yin, K. (2020). "Landslide Displacement Prediction Combining LSTM and SVR Algorithms: A Case Study of Shengjibao Landslide from the Three Gorges Reservoir Area." *Applied Sciences,* 10, 7830.

Keqiang, H., Xiangran, L., Xueqing, Y., and Dong, G. (2008). "The landslides in the Three Gorges Reservoir Region, China and the effects of water storage and rain on their stability." *Environmental Geology,* 55, 55-63.

Kong, W., Dong, Z.Y., Jia, Y., Hill, D.J., Xu, Y., and Zhang, Y. (2017). "Short-term residential load forecasting based on LSTM recurrent neural network." *IEEE Transactions on Smart Grid*, 10, 841-851.

Lee, T.-S., and Chen, I.F. (2005). "A two-stage hybrid credit scoring model using artificial neural networks and multivariate adaptive regression splines." *Expert Systems with Applications,* 28, 743-752.

Li, D., Yin, K., and Leo, C. (2010). "Analysis of Baishuihe landslide influenced by the effects of reservoir water and rainfall." *Environmental Earth Sciences*, 60, 677-687.

Lian, C., Zeng, Z., Yao, W., and Tang, H. (2015). "Multiple neural networks switched prediction for landslide displacement." *Engineering geology,* 186, 91-99.

Sak, H., Senior, A.W., and Beaufays, F. (2014). "Long short-term memory recurrent neural network architectures for large scale acoustic modeling." *Proc. of the Annual Conference of the International Speech Communication Association, INTERSPEECH.*

Smola, A.J., and Schölkopf, B. (2004). "A tutorial on support vector regression." *Statistics and computing*, 14, 199-222.

Sutskever, I., Vinyals, O., and Le, Q.V. (2014). "Sequence to sequence learning with neural networks." *Advances in neural information processing systems*, 27, 3104-3112.

Taylor, S.J., and Letham, B. (2018). "Forecasting at scale." *The American Statistician*, 72, 37-45.

Wang, F.-W., Zhang, Y.-M., Huo, Z.-T., Matsumoto, T., and Huang, B.-L. (2004). "The July 14, 2003 Qianjiangping landslide, three gorges reservoir, China." *Landslides*, 1, 157-162.

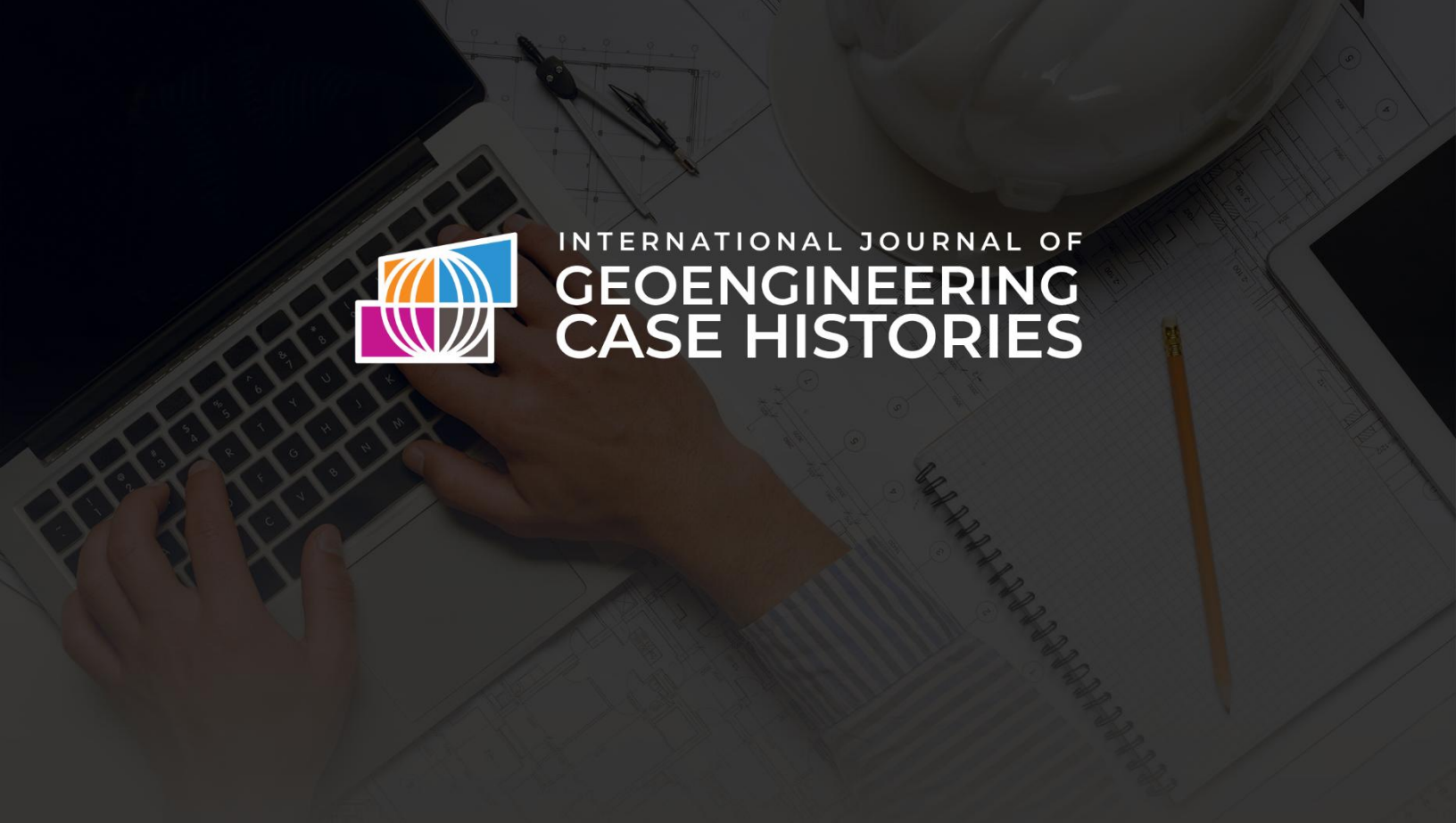
Wang, L., Tang, L., Wang, Z., Liu, H., and Zhang, W. (2020a). "Probabilistic characterization of the soil-water retention curve and hydraulic conductivity and its application to slope reliability analysis." *Computers and Geotechnics*, 121, 103460.

Wang, L., Wu, C., Tang, L., Zhang, W., Lacasse, S., Liu, H., and Gao, L. (2020b). "Efficient reliability analysis of earth dam slope stability using extreme gradient boosting method." *ACTA GEOTECHNICA*.

Weytjens, H., Lohmann, E., and Kleinsteuber, M. (2019). "Cash flow prediction: MLP and LSTM compared to ARIMA and Prophet." *Electronic Commerce Research*, 1-21.

Xie, P., Zhou, A., and Chai, B. (2019). "The application of long short-term memory (LSTM) method on displacement prediction of multifactor-induced landslides." *IEEE Access*, 7, 54305-54311.

Xing, Y., Yue, J., Chen, C., Cong, K., Zhu, S., and Bian, Y. (2019). "Dynamic displacement forecasting of dashuitian landslide in china using variational mode decomposition and stack long short-term memory network." *Applied Sciences*, 9, 2951.
Xu, S., and Niu, R. (2018). "Displacement prediction of Baijiabao landslide based on empirical mode decomposition and long short-term memory neural network in Three Gorges area, China." *Computers & Geosciences*, 111, 87-96.
Yan, J., Wang, L., Song, W., Chen, Y., Chen, X., and Deng, Z. (2019). "A time-series classification approach based on change detection for rapid land cover mapping." *ISPRS Journal of Photogrammetry and Remote Sensing*, 158, 249-262.
Yang, B., Yin, K., Lacasse, S., and Liu, Z. (2019). "Time series analysis and long short-term memory neural network to predict landslide displacement." *Landslides*, 16, 677-694.
Yin, Y., Wang, H., Gao, Y., and Li, X. (2010). "Real-time monitoring and early warning of landslides at relocated Wushan Town, the Three Gorges Reservoir, China." *Landslides*, 7, 339-349.
Zhang, W., and Goh, A.T.C. (2016). "Multivariate adaptive regression splines and neural network models for prediction of pile drivability." *Geoscience Frontiers*, 7, 45-52.
Zhang, W., Tang, L., Li, H., Wang, L., Cheng, L., Zhou, T., and Chen, X. (2020a). "Probabilistic stability analysis of Bazimen landslide with monitored rainfall data and water level fluctuations in Three Gorges Reservoir, China." *Frontiers of Structural and Civil Engineering*, 1-15.
Zhang, W., Zhang, R., Wu, C., Goh, A.T.C., Lacasse, S., Liu, Z., and Liu, H. (2020b). "State-of-the-art review of soft computing applications in underground excavations." *Geoscience Frontiers*, 11, 1095-1106.
Zhang, W.G., and Goh, A.T.C. (2013). "Multivariate adaptive regression splines for analysis of geotechnical engineering systems." *Computers and Geotechnics*, 48, 82-95.
Zhang, W.G., Li, H.R., Wu, C.Z., Li, Y.Q., Liu, Z.Q., and Liu, H.L. (2020c). "Soft computing approach for prediction of surface settlement induced by earth pressure balance shield tunneling." *Underground Space*.
Zhang, Y., Wang, X., and Tang, H. (2019). "An improved Elman neural network with piecewise weighted gradient for time series prediction." *Neurocomputing*, 359, 199-208.
Zhou, C., Yin, K., Cao, Y., and Ahmed, B. (2016). "Application of time series analysis and PSO–SVM model in predicting the Bazimen landslide in the Three Gorges Reservoir, China." *Engineering geology*, 204, 108-120.
Zhou, C., Yin, K., Cao, Y., Ahmed, B., Li, Y., Catani, F., and Pourghasemi, H.R. (2018). "Landslide susceptibility modeling applying machine learning methods: A case study from Longju in the Three Gorges Reservoir area, China." *Computers & Geosciences*, 112, 23-37.
Zhou, Y., and Leung, H. (2007). "Predicting object-oriented software maintainability using multivariate adaptive regression splines." *Journal of systems and software*, 80, 1349-1361.
Zunic, E., Korjenic, K., Hodzic, K., and Donko, D. (2020). "Application of Facebook's Prophet Algorithm for Successful Sales Forecasting Based on Real-world Data."



INTERNATIONAL JOURNAL OF
GEOENGINEERING
CASE HISTORIES

The Journal's Open Access Mission is generously supported by the following Organizations:

dar
a Sidara company

Geosyntec consultants
engineers | scientists | innovators

CONETEC
MUD BAY DRILLING
LANKELMA
Geotech DRILLING

ENGEO
Expect Excellence

Access the content of the ĪSSMGE Īnternational Journal of Geoengineering Case Histories at:
www.geocasehistoriesjournal.org

Downloaded: Wednesday, November 11 2026, 12:23:04 UTC